



HAL
open science

Acoustical Surface Characterization of PP/OWF Composite Plates

Nesrine Bouhamed, Pierre Marechal, Olivier Lenoir, Jean Duclos, Slim
Souissi, Mohammed Ben-Amar

► **To cite this version:**

Nesrine Bouhamed, Pierre Marechal, Olivier Lenoir, Jean Duclos, Slim Souissi, et al.. Acoustical Surface Characterization of PP/OWF Composite Plates. Forum Acusticum 2020, Dec 2020, Lyon (en ligne), France. 10.48465/fa.2020.0115 . hal-03097105

HAL Id: hal-03097105

<https://hal.science/hal-03097105>

Submitted on 5 Jan 2021

HAL is a multi-disciplinary open access archive for the deposit and dissemination of scientific research documents, whether they are published or not. The documents may come from teaching and research institutions in France or abroad, or from public or private research centers.

L'archive ouverte pluridisciplinaire **HAL**, est destinée au dépôt et à la diffusion de documents scientifiques de niveau recherche, publiés ou non, émanant des établissements d'enseignement et de recherche français ou étrangers, des laboratoires publics ou privés.

Acoustical Surface Characterization of PP/OWF Composite Plates

Nesrine Bouhamed^{1,2}, Pierre Maréchal¹, Olivier Lenoir¹, Jean Duclos¹,
Slim Souissi², Mohammed Ben-Amar²

¹ LOMC, UMR CNRS 6294, Normandy University of Le Havre, France

² LASEM, ENIS, University of Sfax, Tunisia

Correspondence: pierre.marechal@univ-lehavre.fr

ABSTRACT

Polypropylene polymer (PP) combined with olive wood flour (OWF) reinforcement is studied in view to find an optimum of viscoelastic properties. The flour ratio content is varied from 0 to 30% and its influence is characterized in terms of surface homogeneity and in terms of acoustic impedance. This acoustical surface property is closely related to the wavelength and active area of the used transducer if it is a plane one. In case of a focused transducer, the wavelength is also a key parameter as well as the so-called f-number which is the ratio between focal distance and active diameter. The focal spot size is thus the surface from which the average acoustical impedance property can be evaluated. The effective wave velocity is deduced from time-of-flight measurements and combined with the average acoustical impedance in order to deduce the effective surface averaged density. As a result, some C-scans of specular echoes obtained for a given PP/OWF composition are compared as a function of the center frequency. The distribution of these acoustical surface properties is compared and discussed for various compositions, depending on the chosen transducer. The influence of the surface roughness is also discussed as an influencing parameter. The analysis of those experimental results constitutes a tool for the improvement of the fabrication process.

1. INTRODUCTION

In Tunisia, the olive tree production generates unused and discarded products that can become environmental pollution. As a solution, the agricultural valorization of olive wood waste led to consider it as a reinforcement in polymers, what constitutes the so-called wood-polymer composites (WPC). The olive wood flour (OWF) constitutes a load made of natural fibers [1] [2] [3], that can be coupled with glass and carbon fibers, contributing to lower cost, higher specific modulus, lighter weight, higher availability and biodegradability [4] [5] [6]. Among various polymers, a thermoplastic one such as the polypropylene (PP) offers many qualities for the fabrication and performance/cost trade-off. The combination of the PP matrix and OWF load has been investigated as an improved WPC material compared to the matrix alone [7]. As a result, the mechanical properties are improved in terms of rigidity through its effective Young's modulus. Nevertheless, the homogeneity of the fabricated samples is always a subject of discussion and of studies.

As a mean of inspection and characterization method, ultrasound non-destructive testing (NDT) offers many advantages [8] relatively to destructive mechanical tests.

As an illustration, the ultrasonic method has been used for the characterization of a WPC by El-Sababagh et al. [8]. The porosity level of a biocomposite material has been estimated by acoustical absorption with a good correlation with mechanical methods as demonstrated by Merotte et al. [10]. In particular, the longitudinal and transverse ultrasonic velocities can be related to the mechanical elastic moduli [12].

Thus, in this work a set of WPC samples made of PP/OWF are studied [13]. The approach developed consists in the evaluation of the homogeneity of those samples. In this view, a local estimation of the acoustical properties is carried out, based on a pulse-echo measurement in a scanning area. These results are then analyzed as a possible evaluation of the surface acoustical impedance, and discussed in terms of surface absorption through surface porosity, surface roughness, or a combination of both phenomena.

2. WOOD-POLYMER COMPOSITES

2.1 WPC samples

The studied WPC samples are those characterized in a previous work [7] in order to deduce their effective acoustical bulk properties. As a result, a set of WPC has been obtained with an increasing charge load, i.e. PP/OWF with a OWF mass loading rate of 0, 10, 20 and 30%. The thickness of those plates is chosen at $d_p = 4$ mm to avoid echo overlapping with a transducer having a gaussian bandwidth of 80% and a 5 MHz center frequency. The lateral dimensions are a width $l = 100$ mm and length $L = 120$ mm, but the analyzed area is reduced to 20×20 mm².

Figure 1 (a) shows the surface of a WPC plate denoted as PP/OWF30, i.e. with a 30% OWF content. One can clearly observe some heterogeneities at a fraction of millimeter scale. Nevertheless, those sample plates are characterized as if they were homogeneous and isotropic.

In Figure 1 (b), the roughness of the plate is illustrated along a line measured horizontally in the center of the analyzed area of 20×20 mm². As it can be observed, the surface roughness presents some variations of several tens of microns. Those surface irregularities may lead to perturbations regarding the classical assumptions used for the wave propagation, i.e. the plane wave assumption and the corollary of canonical geometries.

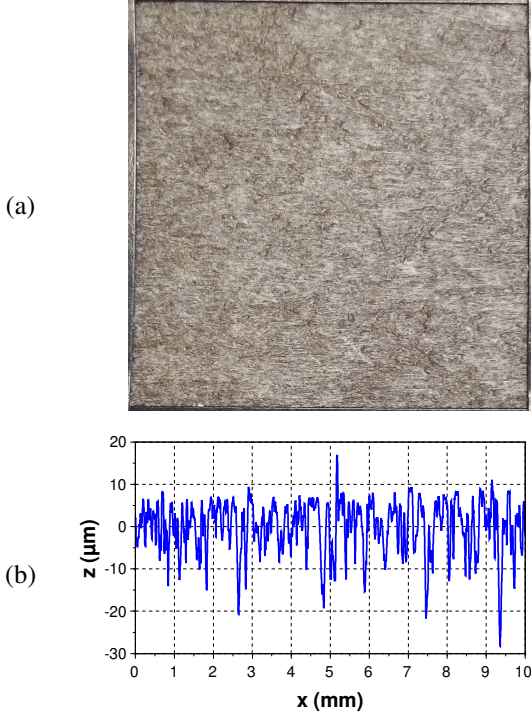


Figure 1. (a) Photo of the studied area of 20×20 mm² and (b) plot of the roughness measured along the horizontal axis in the center of the PP/OWF30 studied area.

2.2 Acoustical properties

On the basis of previous works [13] [7], a classical weighting of the samples leads to the density ρ , a time-of-flight estimate through the thickness gives the longitudinal wave velocity c_L , and a reflection spectrum approach at oblique incidence delivers the transverse wave velocity c_T . These measured values have all been estimated with a relative error of 3% and are summarized in Table 1:

m_{FBO} (%)	0	10	20	30
ρ (kg/m ³)	905	928	953	979
c_L (m/s)	2600	2640	2680	2720
c_T (m/s)	1230	1270	1310	1320

Table 1. Experimental values of the acoustical properties of WPC made of PP/OWF as a function of the OWF mass fraction m_{OWF} (%).

3. ACOUSTICAL IMPEDANCE

The acoustical impedance is related to the bulk properties of the plate, but also to its interface with the surrounding medium. As a result, the acoustic impedance depends on its definition, i.e. $Z = \rho \cdot c_L$, but also on the way it is evaluated. In the case of a standard measurement based on a classical density defined as the ratio $\rho = m/V$ between the mass m and volume V of the studied sample, and a longitudinal wave velocity is evaluated using the ratio $c_L = 2d/\tau$ between the thickness d and time-of-flight τ .

3.1 Assumptions

This definition of the acoustical impedance assumes many hypothesis such as the sample homogeneity, and ideal geometry of the sample with perfectly flat and parallel faces in the scanning area, as well as negligible or compensated diffraction effects [14]. A simple geometric approach of the problem remind those estimates are resulting from average geometrical effects:

$$\begin{cases} \bar{\rho} = \frac{1}{V} \iiint_V \rho(V) \cdot dV \\ \bar{c}_L = \frac{1}{S} \iint_S D_S \cdot \left(\frac{1}{d} \int_d c_L(z) \cdot dz \right) \cdot dS \end{cases} \quad (1)$$

where V , S , d are the volume, surface and thickness insonified at the top face of the plate respectively, and D_S is the normalized surface relative diffraction correction. In a far-field approximation, this D_S diffraction correction is the Fourier transform of the source geometry [15], resulting in a weighted spatial average estimate.

3.2 Pulse-echo reflectometry

An alternative to this method consists in using the reflection coefficient to evaluate the acoustical impedance. This method is based on the plane-wave assumption, reflection on a perfectly flat surface and homogeneity of the insonified medium. With a pulse-echo measurement at normal incidence, under the assumption of the stability of the experimental environment, Gururaja et al. [16] demonstrated that the echo amplitude of the specular echo can be directly related to the reflection coefficient between the plate and the immersion medium:

$$s_0(t) = s_{ref}(t - \tau_w) \cdot D_w \cdot R_{wp} \quad (2)$$

where $s_{ref}(t)$ is the reference echo directly at the output of the transducer, τ_w is a time-of-flight resulting from a round-trip between the transducer and the plate, D_w is the correction factor integrating both diffraction effect and attenuation in water and R_{wp} is the reflection coefficient at the interface between water and the plate.

Then, the reflection coefficient can be deduced from the equation (2), using the echo of interest $s_0(t)$ and the reference echo $s_{0,ref}(t)$ obtained in the same experimental and operating conditions. Thus, the reflection coefficient of the studied plate R_{wp} can be deduced from that of a well-known reference medium $R_{wp,ref}$ as follows:

$$R_{wp} = R_{wp,ref} \frac{\max\{s_0(t)\}}{\max\{s_{0,ref}(t)\}} \quad (3)$$

Therefore, the acoustical surface impedance of the plate Z_{ps} can be deduced from this reflection coefficient R_{wp} as follows:

$$Z_{ps} = Z_w \frac{1 - R_{wp}}{1 + R_{wp}} \quad (4)$$

As a reminder, this acoustical surface impedance Z_{ps} is formally different from that of the classical definition, involving homogenous values of the density and velocity in the whole volume. Here, the acoustical surface impedance Z_{ps} only refers to the values in the vicinity of the top surface. This make it difficult to extract the local density, since the velocity may be known spatially, but still results from a time-of-flight along the whole thickness.

4. METHOD

4.1 Experimental setup

For the local ultrasonic inspection, the sample plate was immersed in a water tank (Figure 2). In this study, the acoustical reflectometry of the plate was performed using an experimental apparatus constituted of a 3D translation thanks to motorized units, controlled by a driving and acquisition device using the UTWin processing software. All the setup apparatus, hardware and software were provided by Mistras. The water tank is kept at a constant temperature using a double container system.

The pulse-echo signal is investigated and only a few adjustments are required, such as a reference time-of-flight τ_v and normal incidence of the ultrasonic beam to the plate.

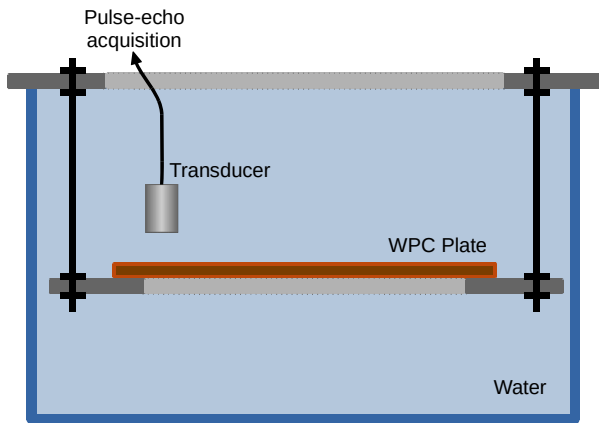


Figure 2. Experimental setup used for the acoustical surface characterization of the studied WPC plates.

4.2 Signal processing

The pulse-echo signals are recorded for each inspection position, defined with a translation step of $100\ \mu\text{m}$, all over the analyzed area of $20 \times 20\ \text{mm}^2$. For each scanning position (x, y) of the studied area, i.e. 201×201 points, the acoustical surface impedance can be deduced from the echo $s_0(t)$ as described in the previous section.

Therefore, for heterogeneous materials, the specular echo gives an image of the reflection coefficient at the interface between water and the WPC plate, and thus of the acoustic impedance of the surface Z_{ps} .

As a result, using equation (4), the acoustical surface impedance Z_{ps} can be deduced for each scanning position (x, y) , and gives a local image of the product density by longitudinal wave velocity at the vicinity of the top face of the WPC plate.

5. RESULTS AND DISCUSSION

5.1 Raw data

The area of analysis was scanned, providing a C-scan map of 201×201 points. The raw data obtained for a pure PP plate (Figure 3 (a)) shows a homogeneous value, but varies between 44 and 48% of the calibrated amplitude, with an average value at 46%, i.e. a 4% relative variation.

In the same experimental and operating conditions, the raw data obtained for PP/OWF10 plate (Figure 3 (b)) shows heterogeneous values, with strong variations from less than 10% up to more than 90%, what can be explained by the composition of the WPC in its volume (and in the vicinity of its faces) and by the roughness of its surface as illustrated in Figure 1 (b).

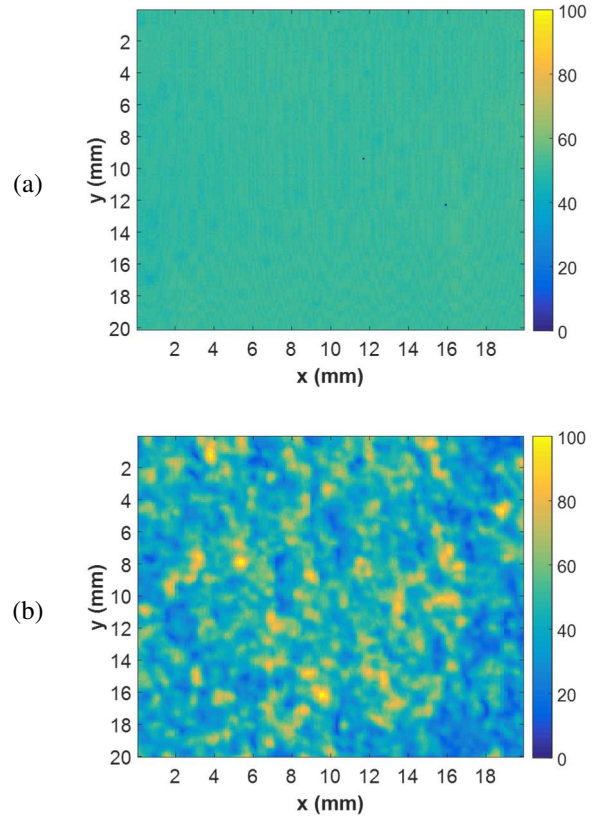


Figure 3. C-scans of the specular echoes obtained on the studied area of $20 \times 20\ \text{mm}^2$ for (a) a pure PP plate and (b) a WPC made of a PP/OWF10 composition.

5.2 Acoustical surface impedance

A processing of these maps as described in equations (3) and (4) gives a C-scan of the acoustical surface impedance (Figure 4). If the WPC plates were or could be considered as homogenous, the C-scan maps would present an acoustical surface impedance close to that resulting from the volume (equation (1)). In the studied set of WPC samples, for OWF = 0, 10, 20 and 30%, we have $Z_p = 2.35, 2.45, 2.55$ and $2.66\ \text{MRa}$, respectively. Similar values would be obtained at the surface if the assumption of homogeneity would have been verified, what means an acoustical impedance of $Z_p = 2.55\ \text{MRa}$ for a WPC made of a PP/OWF20 composition.

Nevertheless, in the present study, many preliminary assumptions are not being strictly verified, but this method can advantageously be used to evaluate the heterogeneity level and roughness estimators.

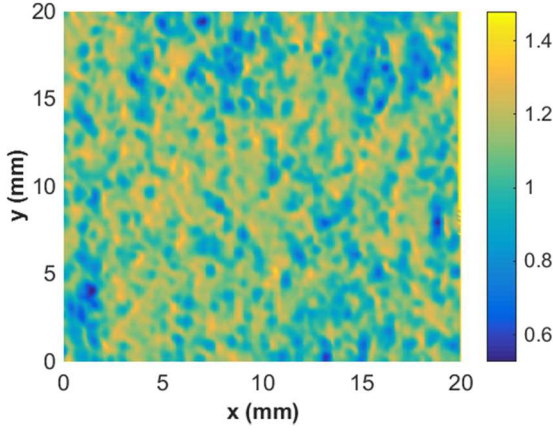


Figure 4. C-scan of the acoustical surface impedance Z_{ps} (MRa) of a PP/OWF20 WPC plate on the studied area of $20 \times 20 \text{ mm}^2$.

As illustrated by Figure 4, strong local variations are observed experimentally, with a mean value of $Z_{ps} = 1.10$ MRa and extrema at 0.57 and 1.48 MRa. This is an apparently disappointing result, with a ratio $Z_{ps}/Z_p = 0.43$ between the expected value in the volume and that of the surface. That disagreement must be discussed.

5.3 Discussion

As it was highlighted in Figure 1, showing the rough surface aspect, the reflection surface does not present a homogenous and perfectly plane face. On the basis of the experimental results and the measured roughness of the surface, the assumption of micro air bubbles at the surface is the most likely assumption. In particular, in the case of an immersion of the sample plate, micro bubbles of air may stay captive in the roughness interstices. Following that hypothesis, a fraction of the insonified surface denoted as $0 \leq p \leq 1$ relates the reflection coefficients implied:

$$R_{wps} = p.R_{wa} + (1-p)R_{wp} \quad (5)$$

where R_{wps} is the reflection coefficient between water and the plate surface and R_{wa} is the reflection coefficient between water and air. As a result, the inverse problem gives an estimate of p , the air surface fraction of the studied sample. Thus, the equation (5) becomes:

$$p = \frac{R_{wps} - R_{wp}}{R_{wa} - R_{wp}} \quad (6)$$

Reciprocally, equations (4) and (5) lead to:

$$Z_{ps} = Z_w \frac{1 - R_{wps}}{1 + R_{wps}} \approx \frac{(1-p)Z_w Z_p}{Z_w + pZ_p} \quad (7)$$

As a result, the normalized acoustical surface impedance Z_{ps}/Z_p is a function of p the air surface fraction, Z_w and Z_p the acoustical impedances of water and of the plate, respectively.

In the case of the studied WPC sample made of a PP/OWF20 composition (Figure 5), the ratio $Z_{ps}/Z_p = 0.43$ gives an average value of $p = 33\%$ of air at the surface of the plate, and extrema at $p_{\max} = 56\%$ and $p_{\min} = 21\%$ for $Z_p = 0.57$ and 1.48 MRa, respectively.

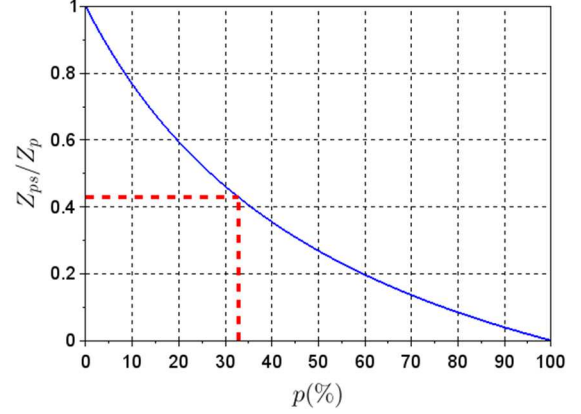


Figure 5. Normalized acoustical surface impedance Z_{ps}/Z_p as a function of the air part p , with $Z_p = 2.55$ MRa for a PP/OWF20 WPC plate and $Z_w = 1.48$ MRa.

Among the critical items, it can be noted that the chosen translation step for the ultrasonic measurement is nearly the same as the mean value of the OWF granulometry distribution around $110 \mu\text{m}$. In addition, the surface roughness can be clearly observed when the load charge exceeds 15%. Eventually, the WPC samples does not appear flat when the load charge of WPC exceeds 20%: one can feel asperities at the surface, constituting an additional variation.

6. CONCLUSION

In this work, the feasibility of the acoustical surface impedance was demonstrated. The method was described as well as the associated assumptions. The experimental setup was presented and some results were shown and discussed. The case of study of a WPC made of a PP/OWF20 composition illustrates the results obtained with the reflectometry method. A significant discrepancy was observed between the acoustical impedance evaluated from a classical density and longitudinal wave velocity measurements, and the reflectometry method which only involves the acoustical properties at the vicinity of the surface of the sample. Similar results have been observed with the other WPC compositions. Further work and investigations are necessary to qualify the surface roughness through the acoustical surface impedance. The strong local variations observed experimentally are to be analyzed more deeply and may be correlated to the local value of the surface roughness, where the air caption is at the moment supposed to occur.

7. REFERENCES

- [1] K. Oksman, «Mechanical properties of natural fibre mat reinforced thermoplastic,» *Applied Composite Materials*, vol. 7, pp. 403-414, 01 11 2000.
- [2] J. Biagiotti, D. Puglia et J. M. Kenny, «A review on natural fibre-based composites - Part I,» *Journal of Natural Fibers*, vol. 1, pp. 37-68, 2004.
- [3] D. Puglia, J. Biagiotti et J. M. Kenny, «A review on natural fibre-based composites - Part II,» *Journal of Natural Fibers*, vol. 1, pp. 23-65, 2005.
- [4] B. Amar, K. Salem, D. Hocine, I. Chadia et M. J. Juan, «Study and characterization of composites materials based on polypropylene loaded with olive husk flour,» *Journal of Applied Polymer Science*, vol. 122, pp. 1382-1394, 2011.
- [5] H. Djidjelli, D. Benachour, A. Boukerrou, O. Zefouni, J. Martinez-Vega, J. Farenc et M. Kaci, «Thermal, dielectric and mechanical study of poly(vinyl chloride)/olive pomace composites,» *eXPRESS Polymer Letters*, vol. 1, n° 112, pp. 846-852, 2007.
- [6] K. Qiu et A. N. Netravali, «Fabrication and characterization of biodegradable composites based on microfibrillated cellulose and polyvinyl alcohol,» *Composites Science and Technology*, vol. 72, pp. 1588-1594, 2012.
- [7] N. Bouhamed, S. Souissi, P. Marechal, M. B. Amar, O. Lenoir, R. Leger et A. Bergeret, «Ultrasound evaluation of the mechanical properties as an investigation tool for the wood-polymer composites including olive wood flour,» *Mechanics of Materials*, vol. 148, p. 103445, 2020.
- [8] T. Kundu, Éd., *Ultrasonic and Electromagnetic NDE for Structure and Material Characterization Engineering and Biomedical Applications*, 2013, pp. 1-877.
- [9] A. El-Sabbagh, L. Steuernagel et G. Ziegmann, «Ultrasonic testing of natural fibre polymer composites: effect of fibre content, humidity, stress on sound speed and comparison to glass fibre polymer composites,» *Polymer Bulletin*, vol. 70, pp. 371-390, 2013.
- [10] J. Merotte, A. Le Duigou, A. Bourmaud, K. Behlouli et C. Baley, «Mechanical and acoustic behaviour of porosity controlled randomly dispersed flax/PP biocomposite,» *Polymer Testing*, vol. 51, pp. 174-180, 2016.
- [11] J. Merotte, A. Le Duigou, A. Bourmaud, K. Behlouli et C. Baley, «Influence du taux de porosité sur les propriétés d'un composite non tissé lin/PP - Porosités dans les biocomposites non tissés,» *Matériaux & Techniques*, vol. 104, pp. 1-11, 2016.
- [12] M. Scalerandi, A. S. Gliozzi, C. L. E. Bruno et P. Antonaci, «Nonequilibrium phenomena in damaged media and their effects on the elastic properties,» *Journal of the Acoustical Society of America*, vol. 131, pp. 4304-4315, 2012.
- [13] N. Bouhamed, S. Souissi, P. Maréchal, M. Ben Amar, O. Lenoir, R. Leger et A. Bergeret, «Caractérisation ultrasonore et mécanique d'un matériau bio-composite à base de farine de bois d'olivier et de polypropylène,» chez *Congrès Français d'Acoustique*, pp. 763-769, Le Havre, 2018.
- [14] N. Ghodhbani, P. Maréchal et H. Duflo, «Ultrasonic broadband characterization of a viscous liquid: Methods and perturbation factors,» *Ultrasonics*, vol. 56, pp. 308-317, 2015.
- [15] T. L. Szabo, *Diagnostic Ultrasound Imaging: Inside Out (Second Edition)*, Boston: Academic Press, 2014.
- [16] T. R. Gururaja, W. A. Schulze, L. E. Cross et R. E. Newnham, «Piezoelectric Composite Materials for Ultrasonic Transducer Applications. Part II: Evaluation of Ultrasonic Medical Applications,» *IEEE Transactions on Sonics and Ultrasonics*, vol. 32, pp. 499-513, 7 1985.